Ju Tang, Jiagui Tao, Xiaoxing Zhang, Jiabin Zhou

State Key Laboratory of Power Transmission Equipment and System Safety and New Technology, College of Electrical Engineering, Chongqing University, Shapingba District, Chongqing 400044, China.

Investigation of Partial Discharge on Typical Defects with UHF Detection Method for GIS

Abstract. *Five typical insulation defect models in 110kV SF_6-insulated switchgear (GIS) are deigned in this paper. Phase Resolved Partial Discharge (PRPD) spectrums for the five defects are constructed by Ultra High Frequency (UHF) method, and a dataset of 390 samples is established. By analysis of the PD distribution, a feature extraction method based on statistical theory is adopted. Finally, fuzzy c-means clustering (FCM) is introduced to analyze the natural similarity among the various typical insulation defects. The results show that the overall recognition rate is of 90.5% high and most of the defects can be roughly unified to their respective categories, except for some intersections of the surface contamination and viod in spacer defects.*

Streszczenie. *W artykule zaproponowano sposób modelowania pięciu typowych uszkodzeń izolacji w rozdzielnicy 110kV SF_6. Przy użyciu techniki fal decymetrowych, opracowano spektra wyładowań niezupełnych, wynikających z pięciu podstawowych defektów. Następnie przy wykorzystaniu analizy statystycznej oraz metody FCM (ang. Fuzzy c-means Clustering) dokonano porównania opisanych defektów. Wyniki pokazują bardzo wysoką skuteczność wykrywania większości awarii, z wyjątkiem niektórych rodzajów zanieczyszczeń powierzchniowych oraz obecności próżni w przekładkach. (**Analiza wyładowań niezupełnych, wynikających z typowych defektów materiałów izolacyjnych w rozdzielniach elektrycznych– detekcja techniką fal decymetrowych**)*

Key words: partial discharge, GIS, typical insulation defects, classification
Słowa kluczowe: wyładowanie niezupełne, rozdzielnica elektryczna, typowe defekty materiału izolacyjnego, klasyfikacja.

Introduction

SF_6-insulated switchgear has many advantages such as minimal space requirements, high safety and reliability, and practically maintenance-free operation [1, 2]. Consequently, its applications have been expanded in the power grid especially in the urban distribution network over the past decade. As GIS plays an increasingly significant role, it is necessary to monitor its running state. Partial discharge (PD) measurement is generally used as an important diagnostic tool for GIS condition monitoring [3, 4], since it can reliably detect incipient faults and provide on-line diagnostic information for condition assessment in real time.

Different types of inner defects contribute negative impacts on the internal insulation in different levels; consequently, recognition of internal insulation defects is very important for GIS operating status assessment [5-8]. In order to obtain the PD characteristics on typical insulation defects of GIS, this paper designs five typical insulation defects on an 110kV GIS device. PRPD spectrums are collected by UHF method, and FCM method is introduced for exploring the regularity of PD on the five defects. Since any prior guide knowledge of the classification is unavailable, and only the similarity between classes and objects is taken as the category sorting criteria, FCM is viewed as an unsupervised classification, which can find the intermediary nature of the sample, and reflect the PD natural attributes objectively. Through observation and analysis of the clustering results, the feasibility of establishment of PD automatic identification system is verified, which lays a foundation for a better identification method.

Experimental equipment and method

PD experiment and detection

The test is carried out on a three-phase GIS (ZF-10-126) in a HV hall with size of 60m*47m*38m (heiligt) in Shandong Taikai High Voltage Switchgear Co.Ltd. The hall is electromagnetic shielded and the ambient temperature is about 10℃. Schematic diagram of PD experiment and detection circuit are shown in Fig.1.

In Fig.1, T1 is a column type voltage regulator, T2 is a power frequency testing transformer without partial discharge (YDTCW-1000/2x500), C1/C2 are power frequency capacitor divider & coupling capacitor (TAWF-1000/600), R is a power frequency protecting resistance (GR1000-1/6), A is a UHF sensor with a bandwidth of 500MHz to 3 GHz and centered about 930MHz. The oscilloscope is Tektronix DPO7104 with a bandwidth of 1GHz and 20GS/s sampling rate. The main equipment is shown in Fig.2.

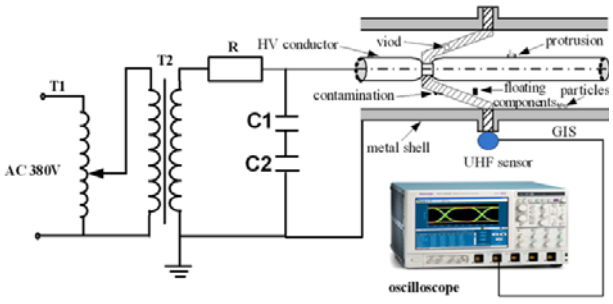

Fig.1 PD Experiment and detection circuit

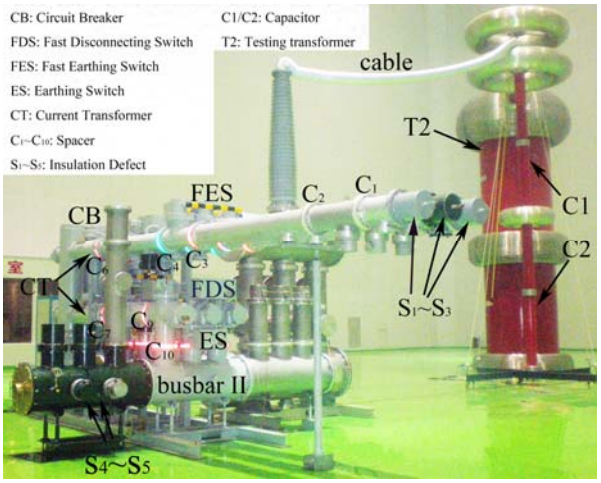

Fig. 2. The main equipment

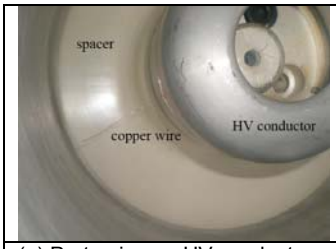

(a) Protrusion on HV conductor

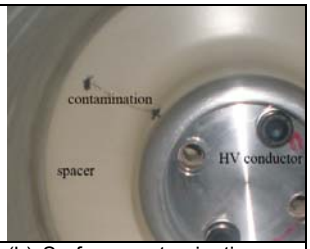

(b) Surface contamination on spacer

(c) Floating components

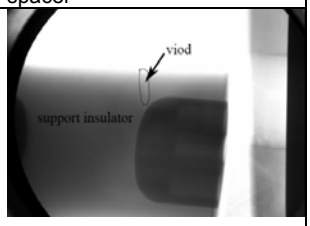

(c) Floating components

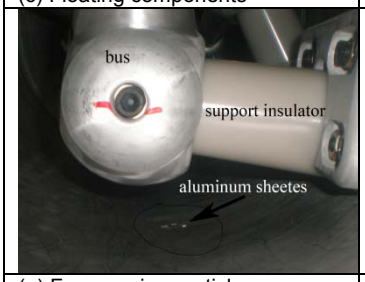

(e) Free moving particles

Fig.3 Five typical defects in GIS

Typical defects and distribution

Five typical insulation defects are designed including protrusion on HV conductor, free moving particles, surface contamination on spacer, viod in spacer and floating components. Fig.3 illustrates all the made up defects. The protrusion defect is simulated using a 2mm diameter copper wire tied on HV conductor with a distance of 40mm to wall of chamber (Fig.3 (a)). The surface contamination defect is simulated using a 2mm diameter copper wire with a distance of 15mm to the HV pole and 35mm to wall of chamber coated on spacer surface (Fig.3 (b)). An 88mm bolt tied on HV conductor by cotton with a distance of about 25mm to both the HV pole and in wall of chamber is used to simulate the floating components defect (Fig.3 (c)), a bad support insulator with a flaw of about 43mm caused by pressure overload is taken as viod in spacer defect (Fig.3 (d)), and the free moving particles defect is simulated using some 2mm*2mm aluminum sheets placed on the bottom of the busbar tank (Fig.3 (e)).

The distribution of defects is shown in Fig.4, where the floating components, surface contamination, and protrusion defects are set close to spacer C_1 separately in three independent air chambers, and the remaining two defects are set in busbar barre II.

In order to weaken the impact of attenuation, refraction and reflection in the process of signal propagation, when detect S_1~S_3 defects, UHF sensors are placed at C_1 spacer, and detection of S_4~S_5, UHF sensors are placed at C_{10} spacer, shown in Fig.5.

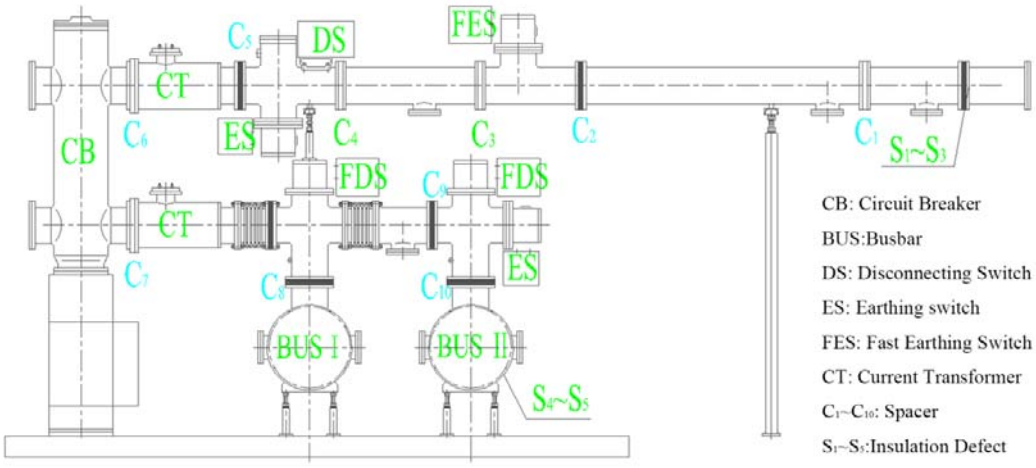

Fig.4 Defects arrangement diagram

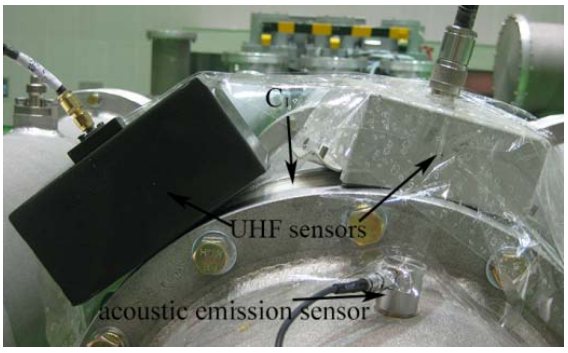

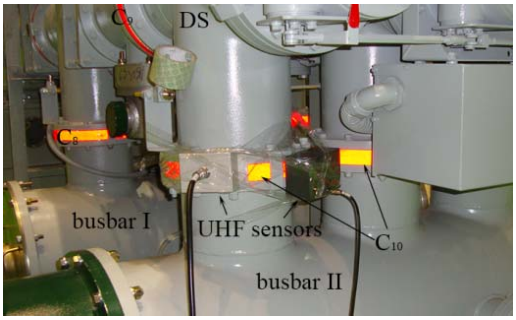

Fig.5 UHF sensors installation

Test voltage application

Only one single defect is conducted each time by some switching operations, when voltage applied. For example, when the single-phase voltage is applied on S_4 via busbar II, just switch off the DS between C_4 and C_5 spacers and switch on the DS above busbar II. The boosting voltage application method [9] is employed in the test. First, select several different test voltage levels and duration time, after the experiment at a given voltage has finished, boost to the next voltage level until the defect is breakdown or is surface flashover. Boosting voltage application is not only capable of modeling the development process of PD, but can also obtain sufficient data within a comparatively short period of time, thus it is more suitable for laboratory testing.

Results and discussion

In this article, a single PRPD sample is composed of PD signals in sequential 50 power cycles (50Hz in China). The sampling rate is set at 50MS/s, and the maximum value of each interval is remained by 2778:1 resampling, which means that a signal data is of 360 points corresponding to a power frequency cycle. Some typical PRPD spectrums are shown in Fig.6.

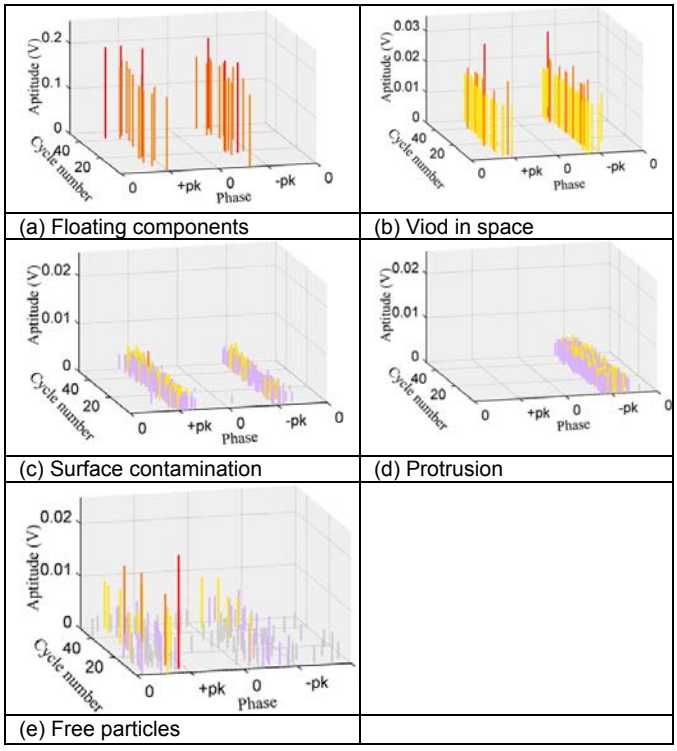

Fig.6 Phase-resolved PD pattern for five insulation defects

Comparing and analysing the PRPD spectrums of five typical defects in Fig.6, we can conclude the following,

Floating components. The PD occurs during the whole power cycle and most of them are before the peak in both positive and negative half-cycles. The amplitude of singal has a maximum value among the five defects and only a little significant difference between in positive and negative half-cycle. With voltage rising, both the amplitude and PD number increases, but the profile of PRPD spectrum is similar.

Surface contamination. The amplitude is relatively small compared to others. When PD just occurs, PRPD spectrum is similar to protrusion defect that PD occurs a little after the peak of negative half-cycle. With voltage rising, PD seldom occurs in positive half-cycle with relatively larger amplitude than in negative half-cycle; when voltage is boosted high enough, PDs are mainly concentrated nearby the peaks in both positive and negative half-cycles and both amplitude and PD number slowly increase.

Viod in spacer. The amplitude of signbal in the positive half-cycle is close to in the negative half-cycle. With voltage rising, PDs are similar in profile and mainly concentrated nearby the peaks in both positive and negative half-cycles.

Protrusion. PD just occurs a little after the peak of the negative half-cycle; when gradually boost the applied voltage, PD seldom occurs in the positive half-cycle with relatively larger amplitude to in the positive half-cycle, both amplitude and PD number increase with a similar profile of PRPD spectrum in the negative half-cycle.

Free particles. Throughout the whole power frequency cycle, the distribution of PD number and amplitude has a strong dispersion and randomness but no obvious polarity effect.

4 Feature extraction

Feature extraction has an important effect on classification. Through observation and analysis of PRPD spectrums, we have found that they are significantly different for five different defects; however whether the mathematical calculations for feature extraction can portray these differences depends on the characteristics calculation method. In order to weaken the influence of feature calculation method on the classification results, we employ classic feature extraction methods based on statistical theory [8,10,11], which are recognized of good calssification ability. All the extracted features are shown inTable.1.

Table.1 Statitical parameters

Index	Features
1-6	Sk_m^+ Sk_m^- Sk_m Sk_n^+ Sk_n^- Sk_n
7-12	Ku_m^+ Ku_m^- Ku_m Ku_n^+ Ku_n^- Ku_n
13-14	Q_m Q_n
15	mcc

*Sk is skewness, Ku is kurtosis, Q is discharge factor, mcc is modified cross correlation factor; m is for amplitude, n is for PD number; + - means the positive and negative half of power frequency cycle

5 FCM for PDs

The extracted features are of 15-dimension, so it is difficult to directly tell the difference of 5 types of defects. Since FCM can find the similarity of objects in natural property and is an unsupervised classification method, we use it for evaluating the classification ability of the PD samples.

5.1 Summarization of FCM

Comparing to other clustering methods, FCM has an advantage that it introduces membership to denote the degree in which a data point belongs to certain types. If the initial cluster centers and the number of clusters are well chosen, it can achieve a high accuracy. By optimizing the objective function, FCM calculates the membership of each sample point on the class center to determine sample points belong to which cluster. FCM is a partitioning algorithm that aims at minimizing the square of the weighted distance of samples to cluster center in each category. Carry it out as follows: let $X=\{x_i,\ i=1,2,\cdots,n\}\in R^s$ stands for a vector which belongs to S-dimensional vector space, and c is a predetermined number of categories. Given $X_1,X_2,\cdots,X_c$ $(2\le c\le n\text{-}1)$, we say that the c fuzzy subsets $\{X\to[0\ \ 1]\ \}$ are a fuzzy c-partition of X if the following conditions on the membership value U_{ik} for the cluster i and the feature vector X_k are satisfied:

$u_{ik} \in [0,1]$, $1 \le i \le c$, $1 \le k \le n$

(1) $\sum_{i=1}^{c} u_{ik} = 1,\ 1 \le k \le n$;

$\sum_{k=1}^{n} u_{ik} > 0, 1 \le i \le c$

Let $v = (v_1, v_2, \ldots, v_c)$ is the cluster center, where $v_i \subset R^s$ is the center of class i $(1 \le i \le c)$, and the FCM objective function can be expressed as:

(2) $J_m(u,v) = \sum_{k=1}^{n}\sum_{i=1}^{c}(u_{ik})^m \|x_k - v_i\|^2$

Where, $\|x_k - v_i\|^2$ is the distance between the sample x_k and cluster centers v_i, generally in Euclidean distance, m is a constant larger than 1 to present the degree of fuzziness. FCM clustering algorithm is some iteration under certain necessary conditions for minimizing J_m $(u,\ v)$ with the following update equations (3-4) [12, 13].

(3) $v_i^* = \frac{\sum_{k=1}^{n}(u_{ik}^*)^m x_k}{\sum_{k=1}^{n}(u_{ik}^*)^m}, i = 1,2,\cdots,c$;

(4) $u_{ik}^* = (\sum_{j=1}^{c}(\frac{\|x_k - v_i\|}{\|x_k - v_j\|})^{2/(m-1)})^{-1}$, $i = 1, 2, \cdots, c$; $k = 1,2, \cdots, n$

FCM clustering algorithm is presented as follows:

Inputs:

X: data set to be clustered;
c: number of clusters;
m: degree of fuzziness;
E_{max}: minimum amount of improvement;

Outputs:

V: matrix of final cluster centers;
U: final fuzzy partition matrix;
J: values of the objective function during iterations;

S1: Fix $2 \le c \le n-1$ and $1 \le m \le +\infty$, and set $k=1$. Give any $E_{max}>0$ and an initial fuzzy c-partition $v=v_1, v_2, \cdots, v_c$

S2: Compute $v^{(k)}$ with $u^{(k-1)}$ by equation (3).

S3: Update $u^{(k)}$ with $v^{(k)}$ by equation (4).

S4: Compare $u^{(k-1)}$ to $u^{(k)}$ in a convenient norm $\|u^{(k-1)} - u^{(k)}\|^2$

IF $\|u^{(k-1)} - u^{(k)}\|^2 < E_{max}$, THEN stop

ELSE $k=k+1$ and return to S2.

5.2 Results and analysis

390 PRPD samples are collected from PD experiment on five typical defects, including 80 groups for protrusion on HV conductor, 88 for free moving particles, 70 for surface contamination on spacer, 80 for viod in spacer and 72 for floating components. Features are extracted by the methods shown in Table.1, before input them to FCM, normalization is quite necessary for avoiding attributes existence in greater numeric ranges dominating over those in smaller numeric ranges and limiting numerical difficulties. In this investigation, the normalization method is explained in formula (5).

(5) $y = \frac{(y\max - y\min) \times (x - x\min)}{(x\max - x\min)} + y\min$

where, y is the normalized value of the input x, $y\max$ is a given maximum value for each normalization output,and $y\min$ is the minimum value, in this paper they are $+1$,-1in several.

Take the normalization result as the input variable X, set $c=5$, $m=2$, $E_{max}=10^{-5}$, and randomly select initial cluster centers, in order to reduce the impact of randomness. The results of the program running five times are as follows:

Values of the objective function during iterations J:

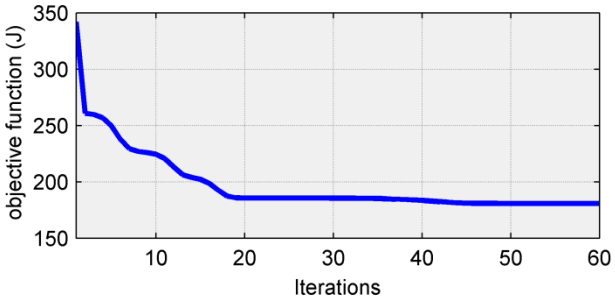

Fig.7 values of the objective function during iterations

The values of the object function are astringent for several times trial, therefore, the final result is not sensitive to the selection of the initial cluster centers in this paper. Since the dimension of final fuzzy partition matrix U is 5*390, we use a competitive transfer function to determine u_i belongs to which type. and the final outcome is shown in Table 2.

Table.2 Recognition results of the algorithm

Type of PDs	Predicted result					Total	Rate
	protrusion	free particles	surface contamination	viod in spacer	floating components		
protrusion	76	0	3	1	0	80	95.0%
free particles	0	86	1	1	0	88	97.7%
surface contamination	4	1	57	7	1	70	81.4%
viod in spacer	1	0	14	65	0	80	81.3%
floating components	1	0	2	0	69	72	95.8%
total	82	87	77	74	70	390	90.5%

The clustering results of FCM are shown in Table.2. We can easily conclude that the overall accuracy of FCM classification is 90.5%, including a higher false rate of surface contamination and viod in spacer defects, and classification of the other three defects has achieved satisfactory results, although it is still with a little error. Furthermore, it is reflected that PDs on the protrusion, free particles and floating components defects have strong regularity, and the distribution of one type of PRPD spectrums is quite similar as the voltage changes and defects ages, while significantly different to each other type. PDs on surface contamination and viod in spacer defects are relatively poor in regularity. Because of the differences on shape, size, ageing degree and location of the two defects, their PRPD spectrums is obviously different to the other three's. Diagnostic accuracy of the two defects is about 81%, thus they can still be used for classification. Maybe a classifier of better performance or some better feature extraction method will improve the classification results.

6 Conclusions

Through a lot of tests, analysis and comparison of PRPD spectrums on five typical defects detection by UHF method in GIS are done. The study found that the distribution characteristics of PRPD spectrums is relatively stable on protrusion, free particles, floating components defects with different applied voltages, and also the contour of the PD distribution for these three defects is obviously dissimilar, but the reminding two defects are fickle.

FCM analysis, with the fifteen feature parameters, is applied to analyze the clustering results for the proposed five typical types of defects. The results show that the overall accuracy of the PD identification can reach up to 90.5%. The discharges in the viod and on the surface of solid insulation can also be distinguished roughly. Since the FCM is an unsupervised classification algorithm and not good at high-dimensional classification, the present classification system can be improved effectively by applying classifier of better performance to establish the automatic identification system.

Acknowledgements. This work was supported by the national key basic research development program—973 under grant No.2009CB724503.

REFERENCES

[1] S. Okabe et al, Propagation Characteristics of Electromagnetic Waves in Three-Phase-Type Tank, *IEEE Transactions on Dielectrics and Electrical Insulation,* 16 (2009), No. 1, 199-205.

[2] X. Zhang et al, Kernel Statistical Uncorrelated Optimum Discriminant Vectors Algorithm for GIS PD Recognition. *IEEE Transactions on Dielectrics and Electrical Insulation*, 16 (2009), No. 1, 206-213

[3] S. Tenbohlen et al, Partial Discharge Measurement in the Ultra High Frequency (UHF) Range, *IEEE Transactions on Dielectrics and Electrical Insulation* 15 (2008), No. 6,1544-1552

[4] W.R.Si, J.H.Li, D.J.Li, et al, Investigation of a Comprehensive Identification Method Used in Acoustic Detection System for GIS, *IEEE Transactions on Dielectrics and Electrical Insulation* 17 (2010),No.3, 721-732,2010.

[5] K.Dreisbusch,H.-G.Kranz and A.Schnettler, Determination of a Failure Probability Prognosis based on PD-Diagnostics in GIS, *IEEE Transactions on Dielectrics and Electrical Insulation* 15 (2008), No.6, 1707-1714

[6] G. C. Stone, Partial Discharge Diagnostics and Electrical Equipment Insulation Condition Assessment, *IEEE Transactions on Dielectrics and Electrical Insulation*, 12 (2005), No. 5, 891-913

[7] S. Okabe et al, Detection of Harmful Metallic Particles inside Gas Insulated Switchgear Using UHF Sensor, *IEEE Transactions on Dielectrics and Electrical Insulation*, 15 (2008), No. 3, 701-709

[8] Sahoo et. al, Trends in Partial Discharge Pattern Classification: A Sur.ey, *IEEE Transactions on Dielectrics and Electrical Insulation* 12 (2005), No. 2, 246-262

[9] QI et al. Severity diagnosi and assessment of the PD provoked by high-voltage electrode protrusion, *IEEE Transactions on power delivery*, 26 (2011), NO. 4, 2363-2369

[10] F.H.Kreuger, et al, classification of Partial Discharges, *IEEE Transactions on Electrical Insulation,* 28 (1993), No.6, 917-931

[11] W.S. Gao, D.W. Ding, and W. D. Liu. Research on the Typical Partial Discharge Using the UHF Detection Method for GIS, *IEEE transaction on power delivery*, 26 (2011) No.4, 2621-2629.

[12] M. Ramze Rezaee, B.P.F. Lelieveldt, J.H.C. Reiber. A new cluster validity index for the fuzzy c-mean, *Pattern Recognition Letters* 19 1998, 237–246

[13] M.S. Yang, Y.J Hua, et al, Segmentation techniques for tissue differentiation in MRI of Ophthalmology using fuzzy clustering algorithms, *Magnetic Resonance Imaging* 20 (2002), 173–179

***Authors**: Jiagui Tao, State Key Laboratory of Power Transmission Equipment & System Security and New Technology, Chongqing University, Chongqing, 400030. E-mail: taojiagui@163.com ; prof. Ju Tang, State Key Laboratory of Power Transmission Equipment & System Security and New Technology, Chongqing University, Chongqing, 400030. E-mail: cqtangju@vip.sina.com; prof. Xiaoxing Zhang, State Key Laboratory of Power Transmission Equipment & System Security and New Technology, Chongqing University, Chongqing, 400030. E-mail: mikezxx@tom.com; Jiabin Zhou, State Key Laboratory of Power Transmission Equipment & System Security and New Technology, Chongqing University, Chongqing, 400030. zhoujb1986@gmail.com.*